

The Molecular Volcano: Abrupt CCl_4 Desorption Driven by the Crystallization of Amorphous Solid Water

R. Scott Smith, C. Huang, E. K. L. Wong, and Bruce D. Kay*

*Environmental Molecular Sciences Laboratory, Pacific Northwest National Laboratory,
P.O. Box 999, Mail Stop K8-88, Richland, Washington 99352*

(Received 3 March 1997)

The desorption kinetics of molecular beam deposited ultrathin films of CCl_4 and amorphous solid water (ASW) are studied. Overlayers of ASW impede CCl_4 desorption until the onset of crystallization, whereupon the CCl_4 desorbs abruptly. The abrupt desorption occurs through connected pathways that are formed in the water overlayer during the nucleation and growth of crystalline ice from ASW. The onset of the abrupt desorption corresponds to the threshold for dynamic percolation. As the crystallization proceeds, the number of connected pathways rapidly increases, giving rise to the episodic release of CCl_4 . [S0031-9007(97)03648-X]

PACS numbers: 81.05.Kf, 61.43.Er, 68.35.Rh, 82.65.-i

Amorphous materials are important in a wide variety of scientific disciplines including physics, chemistry, materials science, and biology [1,2]. Amorphous solid water (ASW) is of special importance for many reasons including the open question over its applicability as a model for liquid water and fundamental interest in the properties of glassy materials [3–5]. Despite the considerable interest in ASW many questions remain about its physical properties, and whether amorphous solid water is a metastable extension of ordinary liquid water or a distinct thermodynamic phase [6–16]. In addition to the properties of ASW itself, understanding the intermolecular interaction between amorphous solid water and an adsorbate is important in such diverse areas as solvation in aqueous solutions, cryobiology, and desorption phenomena in cometary and interstellar ices [14,17,18].

In this Letter we report the observation of abrupt CCl_4 desorption driven by the crystallization of ASW. We term this dramatic effect the “molecular volcano.” The CCl_4 /ASW system was chosen for study because liquid water and CCl_4 are immiscible due to hydrophobic interactions. Water vapor deposited on low temperature substrates (<140 K) is known to form an amorphous phase termed ASW that is metastable with respect to crystalline ice [3,4]. Metastable ASW has a higher free energy than the crystalline ice, and as a result, the water desorption rate from ASW is greater. We have used the difference in the desorption rates to determine the relative free energy of the two phases [13] and to quantitatively study the desorption and crystallization kinetics of ultrathin films of ASW [19,20]. In the experiments described here the desorption kinetics of compositionally tailored, ultrathin films composed of $\text{ASW}(\text{H}_2\text{O})$, $\text{ASW}(\text{D}_2\text{O})$, and CCl_4 are examined using temperature programmed desorption (TPD).

The experimental technique and apparatus have been described elsewhere and are only summarized here [21,22]. In brief, a quadruply differentially pumped

effusive molecular beam of D_2O , H_2O , or CCl_4 was used to dose a 1 cm diameter single crystal metallic substrate [Au(111) or Ru(001)]. This highly collimated beam has a circular profile of ~ 0.35 cm diameter and enables precise and reproducible exposures to be attained without appreciable adsorption on surfaces other than the sample crystal. The beam flux was defined in terms of crystalline ice monolayers where $1 \text{ ML} = 1.06 \times 10^{15}$ molecules/cm². The substrate was prepared, cleaned, and ordered using standard techniques [21,22]. Films of varying composition were prepared by sequential dosing of the 85 K substrate with D_2O , H_2O , or CCl_4 . After film growth, the substrate was resistively heated at a ramp rate of 0.6 K/s from 85 K to a temperature above which the composite film had completely desorbed. A quadrupole mass spectrometer was used to measure the angle-integrated desorption rate as a function of time. The mass spectrometer signals are corrected for mass fragmentation effects that occur during electron impact ionization and are converted to absolute desorption rates in monolayers per second. It is important to note that the diameter of these deposits is approximately 0.35 cm while the height is less than 500 Å. This geometry has about 10^5 times more surface area on the top than on the side, and, as such, desorption from the cylinder wall of the deposit is negligible. The drawings on the figures schematically represent the relative positions of the two components in the composite film. In all cases the CCl_4 desorption kinetics were found to be substrate independent.

Figure 1(a) displays TPD spectra for films where 5.4 ML of CCl_4 is grown on top of a 30 ML film of either H_2O or D_2O ASW at 85 K. In all of the experiments, the CCl_4 film is sufficiently thick to avoid complications in the TPD arising from hydrophobic interactions with the underlying water [23]. Because the CCl_4 desorption rate is much greater than the water desorption rate, the CCl_4 film is completely desorbed prior to the

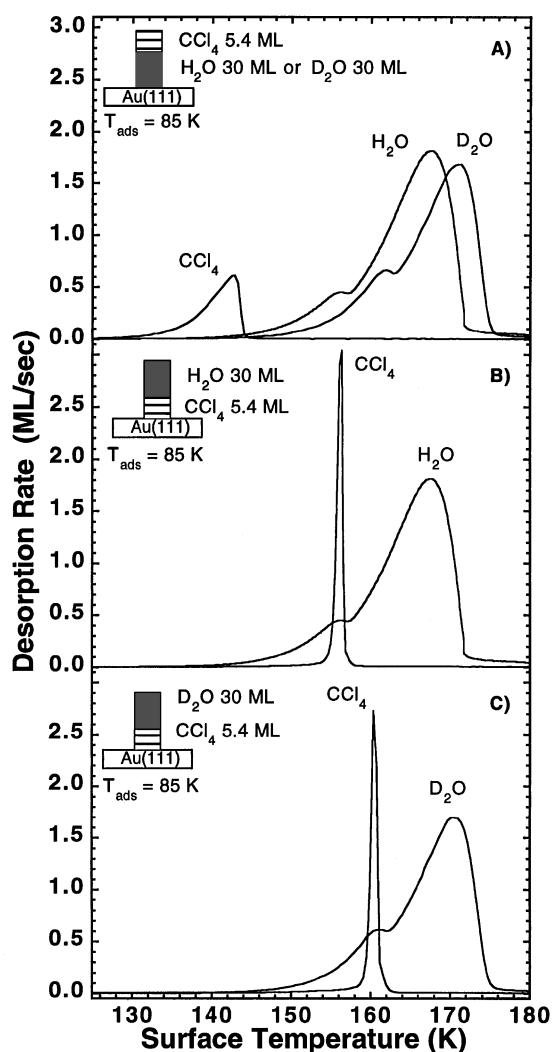


FIG. 1. (a) TPD spectra for nanoscale films of 5.4 ML CCl_4 grown on top of 30 ML of either H_2O or D_2O ASW. The CCl_4 desorption from either ASW substrate is the same. The bump in the water desorption spectra (~ 156 K for H_2O and ~ 161 K for D_2O) arises from the irreversible phase transformation of ASW into crystalline ice. (b) TPD spectra for nanoscale films of ~ 30 ML of ASW(H_2O) grown on top of ~ 5.4 ML CCl_4 . (c) TPD spectra for nanoscale films of ~ 30 ML of ASW(D_2O) grown on top of ~ 5.4 ML CCl_4 . The spectra in both (b) and (c) show that the CCl_4 is trapped beneath the ASW deposit and then desorbs abruptly in concert with the ASW crystallization.

onset of significant water desorption. The CCl_4 desorption is well described by zero-order Arrhenius kinetics, rate = $\nu_0 \exp(-E_d/RT)$, yielding Arrhenius parameters ($E_d \sim 41$ kJ/mole) consistent with unobstructed multilayer sublimation. The water TPD is more complicated and cannot be described by a single rate equation [7,19]. The TPD spectra for H_2O and D_2O are shifted by ~ 5 K reflecting the lower zero point energy of the deuterated ASW. The “bump” in the water desorption spectra (~ 156 K for H_2O and ~ 161 K for D_2O) arises from the

irreversible phase transformation of ASW into crystalline ice. The metastable ASW has a higher free energy and concomitantly higher desorption rate than crystalline ice. Quantitative measurements of the desorption rates from the amorphous and crystalline phases of H_2O and D_2O have been reported previously [13]. The kinetics of the crystallization are discussed in detail elsewhere [19]. For the purpose of this Letter the bump in the water TPD spectrum is the hallmark of the crystallization of ASW [13]. The TPD spectra in Fig. 1(a) are indistinguishable from samples in which CCl_4 and ASW are deposited in spatially separate columns by translating the metallic substrate between doses.

Figures 1(b) and 1(c) display TPD spectra for films where a 30 ML nanoscale film of either H_2O or D_2O ASW is grown on top of 5.4 ML of CCl_4 at 85 K. The TPD spectra show that the CCl_4 desorption is impeded by the ASW overlayer until the onset of crystallization. In concert with the ASW crystallization the underlying CCl_4 desorbs abruptly over a narrow temperature range [$\Delta T(\text{FWHM}) < 1$ K]. The CCl_4 desorption peak shifts to higher temperature (~ 5 K) upon deuteration of the ASW reflecting the isotopic dependence of the crystallization. Collectively these observations suggest that CCl_4 desorption through the ASW overlayer is directly correlated with the amorphous to crystalline phase transition.

Figure 2 displays an Arrhenius plot of the CCl_4 TPD data presented in Fig. 1. The solid lines are the experimental data and the dashed line is an Arrhenius fit to the sublimation of the unobstructed CCl_4 film. The two CCl_4 desorption curves with ASW overlayers exhibit a more complicated temperature dependence. For temperatures below the onset of crystallization the CCl_4 desorption rate is independent of ASW isotope and roughly

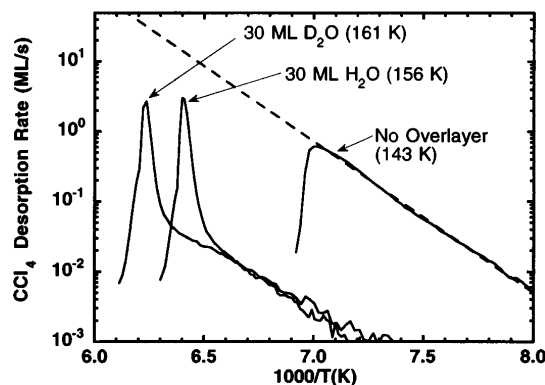


FIG. 2. Arrhenius plot of the CCl_4 desorption rate data in Fig. 1. The three solid lines correspond to desorption from a film with no overlayer, a film with a 30 ML ASW(H_2O) overlayer, and a film with a 30 ML ASW(D_2O) overlayer. The dashed line is an Arrhenius fit to the multilayer desorption part of the CCl_4 desorption curve with no water overlayer. The abrupt change in slope occurs at different temperatures for the H_2O and D_2O overlayers. This difference corresponds to the temperature shift for the onset of the ASW crystallization.

100-fold lower than the free desorption curve. Note that this greatly attenuated desorption is not discernible from the baseline on a linear plot (cf. Fig. 1). At higher temperatures the CCl_4 desorption rate increases rapidly, concurrent with the isotope dependent crystallization of the ASW overlayer. The temperature for the onset of rapid desorption increases by ~ 5 K for the ASW(D_2O) overlayer. Arrhenius analysis of the abrupt desorption region yields an isotope independent apparent activation energy of ~ 500 kJ/mole. As discussed below we do not believe that this large apparent activation energy is associated with any elementary molecular-level activated process.

Further insight into the origin of the complex CCl_4 desorption can be gained by studying the kinetics as a function of the ASW overlayer thickness. Figure 3 displays an Arrhenius plot of the CCl_4 desorption rate from films grown with ASW(D_2O) overlayers of 0, 15, 30, and ≥ 60 ML. As in Fig. 2 the dashed line is an Arrhenius fit to the sublimation of the unobstructed CCl_4 film. The desorption kinetics display a marked dependence upon ASW overlayer thickness. For temperatures below the onset of crystallization the desorption rate decreases with increasing overlayer thickness, reaching an immeasurably small value for overlayers of 60 ML and greater. When detected, this low-temperature desorption occurs with the same apparent activation as free desorption. Although we observe this desorption experimentally, it accounts for removal of only a small fraction ($< 5\%$) of the initial 5.4 ML CCl_4 film.

ASW films grown via vapor deposition are known to be microporous [22]. We believe the low-temperature CCl_4 desorption arises from the existence of a small number of connected pathways in the ASW overlayer formed during ASW deposition at 85 K. As the ASW film is grown thicker, the number of connected pathways that

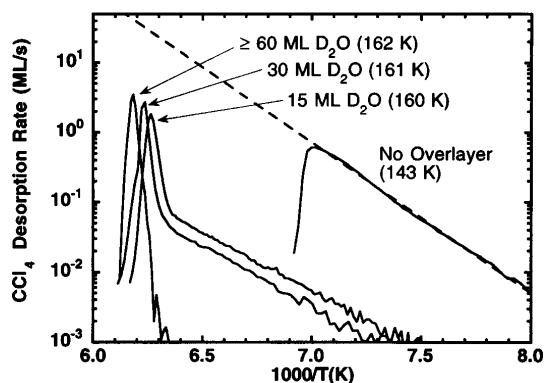


FIG. 3. Arrhenius plot of the CCl_4 desorption rate from nanoscale films with various ASW(D_2O) overlayers (0, 15, 30, ≥ 60 ML). The dashed line is a fit to the curve with no overlayer. The temperature of the abrupt change in slope shifts with the thickness of the overlayer in a manner consistent with the thickness dependence of the ASW crystallization.

traverse the film decreases rapidly to a level below our detection limit for films thicker than 60 ML. Based upon the magnitude of the CCl_4 desorption we estimate that the connected pathway subtends a surface area less than 1% of the unobstructed film for all thicknesses in Fig. 3. As displayed in Fig. 2 this low-temperature desorption is isotope independent for a given film thickness, suggesting isotope independent ASW film growth and morphology.

The plots in Fig. 3 show that the peak temperature for rapid desorption increases with the thickness of the D_2O overlayer, reaching a thickness independent value for overlayers thicker than 60 ML. There is only a 2 K temperature difference in the peak desorption temperature between the 15 and 60 ML experiments. The observation that the peak temperature reaches a saturation value with increasing thickness (60–200 ML) argues against diffusion as the mechanism for the observed abrupt CCl_4 desorption. Although not displayed here, isothermal measurements as a function of film thickness also rule out diffusion because the time associated with the appearance of the molecular volcano saturates with increasing overlayer thickness rather than increasing as the square of the thickness. These observations are completely consistent with the thickness and isotope dependence of the amorphous to crystalline phase transition kinetics [13,19].

Structural changes that occur during crystallization may facilitate the formation of connected desorption pathways in the water overlayer. These pathways can arise from the formation of cracks, fissures, and/or grain boundaries during the nucleation and growth of crystalline ice from ASW. Prior to the formation of these pathways the desorption of CCl_4 through the overlayer is not possible, but at the point a connected pathway is formed, the underlying CCl_4 can begin to escape. As the crystallization proceeds, the number of connected pathways in the overlayer increases giving rise to the abrupt release of CCl_4 observed experimentally. It is important to note that the molecular volcano escape channels are not formed from the pressure the underlying CCl_4 exerts on the ASW overlayer. Arrhenius extrapolation to 162 K yields an unobstructed CCl_4 desorption rate of ~ 100 ML/s corresponding to a pressure of $\sim 10^{-7}$ atm. Based on the ratio of the peak desorption to the Arrhenius extrapolation of the free desorption rate we estimate that these pathways result in an effective desorption area of $\sim 10\%$ of the unobstructed film.

Using isothermal desorption we have observed an induction time for the onset of abrupt desorption. This behavior suggests that a threshold fraction of the ASW must crystallize before a connected path is formed. In the parlance of percolation theory such a threshold corresponds to the onset of dynamic percolation [24,25]. Physically, the CCl_4 escape path is probably formed via grain boundaries produced from the impingement of adjacent crystalline grains growing out of the amorphous

phase or from fractures created by stresses arising from density differences in the amorphous and crystalline phases. Presently we are engaged in experiments aimed at quantitatively correlating the CCl_4 release threshold with the extent of crystallization to further elucidate the mechanism of CCl_4 escape.

Two recent TPD studies on the interaction of a water overlayer with an underlying adsorbate have been reported. Blanchard and Roberts [23] observe a similar temperature shift for the desorption of CCl_4 trapped under an amorphous water layer. They ascribe the observed temperature shift to a diffusional barrier that prevents desorption until a significant amount of the water overlayer has desorbed creating holes in the overlayer. Our experiments clearly demonstrate that the onset of CCl_4 desorption is not related to the amount of the water overlayer that desorbs, but rather is coupled to the phase transition kinetics. Livneh *et al.* [26] report a temperature shift for the desorption of 1 ML of N_2 trapped beneath a water overlayer. In their experiments the desorption of N_2 shifts from 105 (no water overlayer) to 167 K (with 9 ML water overlayer). They attribute this shift to water cages that form around the N_2 . In their model, the desorption of N_2 occurs via site exchange between the N_2 and the water cage. Their observed temperature shift is near the ASW to crystalline ice transition and their results could be equally explained by the mechanism we describe above. Additional experiments are needed to resolve this issue. Neither of the prior studies [23,26] employed water TPD of sufficient resolution to observe the ASW to crystalline transition.

From the evidence outlined above, we demonstrate that the abrupt CCl_4 desorption occurs in concert with the crystallization of the ASW overlayer. The abrupt desorption occurs through connected pathways that are formed in the water overlayer during the nucleation and growth of crystalline ice from ASW. The onset of the abrupt desorption corresponds to the threshold for dynamic percolation [24,25]. As the crystallization proceeds, the number of connected pathways rapidly increases giving rise to the episodic release of CCl_4 . Further details about the dynamics of the microstructural evolution accompanying the crystallization of ASW can be obtained by extending the experiments presented here to include other underlying molecules.

We gratefully acknowledge helpful discussions with S. A. Joyce and G. A. Kimmel. This work was supported by the U.S. Department of Energy Office of Basic Energy Sciences, Chemical Sciences Division. Pacific Northwest National Laboratory is operated for the U.S. Department

of Energy by Battelle under Contract No. DE-AC06-76RLO 1830.

*To whom all correspondence should be addressed.
Electronic address: BD_Kay@PNL.Gov

- [1] C. A. Angell, *Science* **267**, 1924 (1995).
- [2] F. H. Stillinger, *Science* **267**, 1935 (1995).
- [3] M. G. Sceats and S. A. Rice, in *Water A Comprehensive Treatise*, edited by F. Franks (Plenum Press, New York, 1982), Vol. 7, p. 83.
- [4] C. A. Angell, in *Water A Comprehensive Treatise* (Ref. [3]), Chap. 1.
- [5] C. A. Angell, *Annu. Rev. Phys. Chem.* **34**, 593 (1983).
- [6] F. X. Prielmeier, E. W. Lang, R. J. Speedy, and H.-D. Ludemann, *Phys. Rev. Lett.* **59**, 1128 (1987).
- [7] R. J. Speedy and C. A. Angell, *J. Chem. Phys.* **65**, 851 (1976).
- [8] G. P. Johari, *Philos. Mag.* **35**, 1077 (1977).
- [9] J. Maddox, *Nature (London)* **326**, 823 (1987).
- [10] C. M. Sorensen, *Nature (London)* **360**, 303 (1992).
- [11] R. J. Speedy, *J. Phys. Chem.* **96**, 2322 (1992).
- [12] P. G. Debenedetti, in *Physical Chemistry of Aqueous Systems: Meeting the Needs of Industry: Proceedings of the 12th International Conference of Water & Steam*, edited by J. H. J. White, J. V. Sengers, D. B. Neumann, and J. C. Bellows (Begell House, New York, 1995), p. 339.
- [13] R. J. Speedy, P. G. Debenedetti, R. S. Smith, C. Huang, and B. D. Kay, *J. Chem. Phys.* **105**, 240 (1996).
- [14] E. Mayer and R. Pletzer, *Nature (London)* **319**, 298 (1986).
- [15] G. P. Johari, *J. Chem. Phys.* **98**, 7324 (1993).
- [16] G. P. Johari, G. Fleissner, A. Hallbrucker, and E. Mayer, *J. Phys. Chem.* **98**, 4719 (1994).
- [17] A. Kouchi, *Nature (London)* **330**, 550 (1987).
- [18] P. Jenniskens and D. F. Blake, *Science* **265**, 753 (1994).
- [19] R. S. Smith, C. Huang, E. K. L. Wong, and B. D. Kay, *Surf. Sci. Lett.* **367**, L13 (1996).
- [20] P. Löfgren, P. Ahlström, D. V. Chakarov, J. Lausmaa, and B. Kasemo, *Surf. Sci. Lett.* **367**, L19 (1996).
- [21] B. D. Kay, K. R. Lykke, J. R. Creighton, and S. J. Ward, *J. Chem. Phys.* **91**, 5120 (1989).
- [22] D. E. Brown, S. M. George, C. Huang, E. K. L. Wong, K. B. Rider, R. S. Smith, and B. D. Kay, *J. Phys. Chem.* **100**, 4988 (1996).
- [23] J. L. Blanchard and J. T. Roberts, *Langmuir* **10**, 3303 (1994).
- [24] *Percolation Structures and Processes*, edited by G. Deutcher, R. Zallen, and J. Alder (Hilger, Bristol, and The Israel Physical Society, Jerusalem, 1983).
- [25] D. Laufer, E. Kochavi, and A. Bar-Nun, *Phys. Rev. B* **36**, 9212 (1987).
- [26] T. Livneh, L. Romm, and M. Asscher, *Surf. Sci.* **351**, 250–258 (1996).